Microrheological investigation on the local viscosity in the drying droplet of polymer solution

Yudai Tanaka[1], Yoshiyuki Komoda[1], Hiroshi Suzuki[1], Ruri Hidema[2]

Chemical Science and Engineering, Kobe University, Japan

Organization of Advanced Science and Technology, Kobe University, Japan

Tel/Fax 81-78-803-6189, Email: komoda@kobe-u.ac.jp

Introduction

A thin layer of polymer solution or particle dispersion on the surface of solid object is convert to solid film through drying to produce various chemicals. However, undesirable localization or non-uniformity of concentration, which causes various coating defects, is frequently observed. This phenomena is usually described by large evaporation rate of solvent compared with diffusion rate of solute. It is reported that 1-D film thinning model with the considerations of surrounding air flow and solvent evaporation can predict the formation of highly concentrated layer at the drying surface[1]. However, it is hard to obtain physical properties to solve the equations.

Direct measurement methods which can show a keen response to micro structural changes in the wet film are desired to be established. Confocal micro spectroscopy[2] and fluorescent probe technique[3] have been studied to show local concentration of materials in a drying film. On the other hand, rheological measurement is also useful to directly show the mechanical properties of the material under drying so that we can intuitively understand the state of drying film such as "solid-like", "gel-like", "fluid", and so on. A usual rheometers provide rheological bulk information. Meanwhile, micro-rheometry is the method to evaluate the rheological properties of material having the volume of micro or pico litter from the motion of probe particles dispersed in the materials. "Passive" micro-rheometry measures Brownian motion of probe particles, and takes longer time as test fluid is concentrated and becomes viscous. Also, it is not suitable for drying film, the rheological properties of which changes with time. In contrast, "Active" one relies on the controlled external forces, which are applied by optical[4], electrical[5], or magnetic field[6-8]. So far, we reported the micro-rheometry using a magnetic micro-button was applied to measure viscosity change at the surface of polymer solution filled in the trough[9]. We then established another system to measure the change of local rheological properties in transparent materials.

In the present study, we focused on the drying process of a sessile droplet of aqueous solution of a non-volatile component on a glass plate, because this is a miniature system of thin film including edge and surface curvature. We then measured local viscosity change at different positions in the droplet and discuss the effect of drying rate and droplet size on the formation of viscosity distribution.

Experimental Setup

The schematic view of experimental set up is shown in Figure 1. The experimental apparatus is composed of an optical lens tube with an objective lens (50×) and two complementary metal oxide semiconductor (CMOS) cameras for high and low magnification views, a quartz glass cell (10mm × 50mm × 1mm) being squeezed by a pair of electromagnets. The microscopic image of a droplet of test fluid place on the glass cell was captured. In addition, the test cell and electromagnets are mounted on a motorized x-y stage, and the optical microscope system is attached to another motorized z-axis stage, so that it is possible to adjust the focus position of the microscope to any points in a droplet. The strength of the magnetic field was changed by the voltage applied to the electromagnet. The application of magnetic field, the control of motorized stages, and the image capture are all controlled by Labview program running on a PC. The spatial resolution of capture image is 0.15 μm/pixel and the interval between frames is 0.03s.

The right figure of Figure 1 shows the top view of the glass cell and electromagnets. A tiny amount of aqueous dispersion of polystyrene micro-particles containing ferromagnetic component, having the diameter of 6μm and density of $1.1g/cm^3$, (called magnetic particle hereafter) was mixed with test fluid. The magnetic particles are easily dispersed in aqueous solution with the help of carboxyl group modification on its surface. A LED light source placed below the glass cell enables to observe the shape of magnetic particle as a dark circle in a microscopic image. The glass cell was placed between the electromagnets being separated by 12 mm. The distance of magnetic particle from electromagnet is determined from the ratio of the moving speed of magnetic particle when the voltage was applied alternately to each electromagnet.
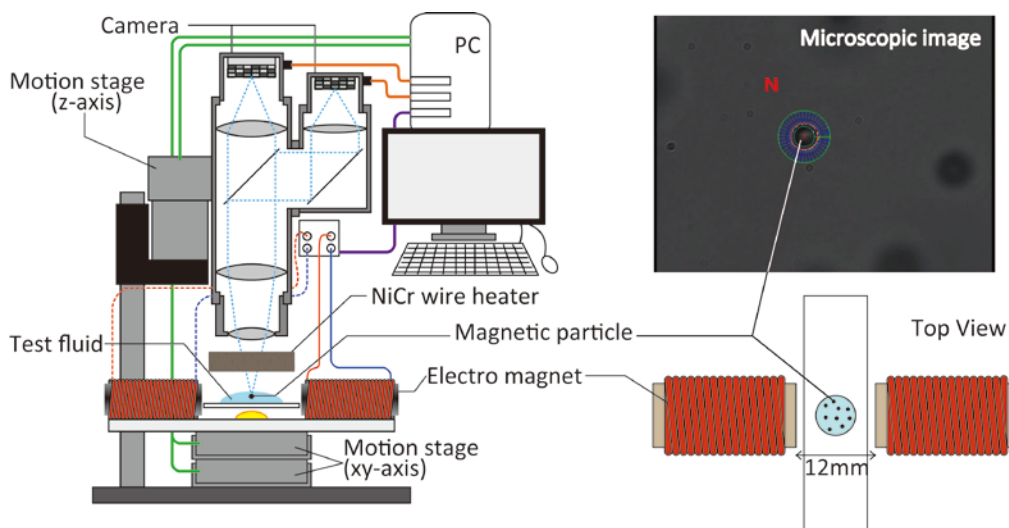

Fig.1 Micro-rheometer setup

A NiCr wire heater was placed between the objective lens and glass cell. The drying condition was changed by the temperature of the heater at 180 or 300ºC. All experiments was carried out

under room temperature and no humidity controlled condition. Since mean inter-particle distance of magnetic particles in a test fluid is on the order of 100μm and the depth of focus is on the order of 1μm, a single magnetic particle is usually observed in a microscopic image without overlapping. Additionally, since sufficient number of magnetic particles are dispersed in a test fluid, at least one magnetic particle is easily found in the field of view at any observation position.

As a test fluid, 6wt% aqueous solution of poly (vinyl alcohol) (PVA) was prepared. The PVA used is partially hydrolyzed and has the degree of polymerization of 2000. The PVA solution was regarded as Newtonian fluid, having the viscosity of 0.04Pa·s.

Viscosity measurement

The speed of a single magnetic particle is determined by the balance between magnetic force caused by non-uniform magnetic field and drag force due to shear stress exerted on the surface of the particle. The effective magnetic force exerted on a single magnetic particle in a test fluid under a magnetic field (magnetic flux density B [T]) is approximated by Eq. (1).

$$F_M = F_p - F_f = \frac{V(\chi_p - \chi_f)}{\mu_0}(B\frac{dB}{dx}) \tag{1}$$

where V[m^3] is the volume of the magnetic particle, and μ_0 [H/m] is the permeability of vacuum (=$4\pi\cdot10^{-7}$ H/m), χ_p, χ_f [-] is the volume magnetic susceptibilities of the magnetic particle and test fluid, x[m] is the distance between the magnetic particle and electromagnet, which generates the magnetic field of interest.

On the other hand, the summation of the drag force on the surface of a single sphere moving in a test fluid must be exerted in the direction opposite to that of the sphere motion. If a single sphere moves sufficiently slowly or a laminar flow is generated around the sphere, the drag force is expressed by the following equation from Stokes's law.

$$F_d = 3\pi\eta d_p v \tag{2}$$

where, η[Pa·s] is the viscosity of the test fluid in the vicinity of the sphere, d_p[m] is the sphere diameter, v[m/s] is the velocity of the sphere. Since the inertia force is negligible in the present study, the balance between F_m and F_d results in the following expression, which was used to calculate the viscosity of the test fluid around the magnetic particles from its moving speed.

$$\eta = \frac{1}{18}\frac{(\chi_p - \chi_f)d_p^2}{\mu_0 v}(B\frac{dB}{dx}) \tag{3}$$

The accuracy and validity of the viscosity measurement using the micro-rheometer described above was checked using aqueous glycerol solutions having various concentrations. The viscosity measurement of these glycerol solutions using a commercial rheometer clearly showed that they all are Newtonian fluids. Also, excellent agreement between the measured viscosities by commercial and our micro rheometers was confirmed as shown in Figure 2.
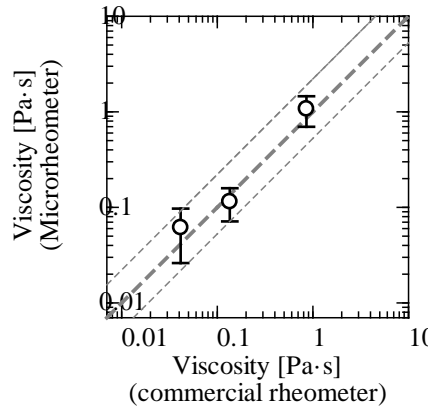
Figure 2 Comparison of viscosities measured using micro-rheometer and commercial bulk rheometer

Determination of droplet size and measurement position

The height of the droplet was measured as the vertical displacement of the z-axis stage from the glass cell surface to droplet top, which is detected by another polystyrene particle attached to the surface. The diameter was measured as the horizontal displacement of the x-y axes stage between edges, which is detected by eyes in microscopic image. The volume of the droplet was calculated as a spherical cap having the height of h and base radius of a as expressed by Eq. (4).

$$V(t) = \frac{\pi}{6}h(t)\{3a(t)^2 + h(t)^2\} \qquad (4)$$

The position of a magnetic particle in a droplet was also determined based on the displacement of motorized stages. The focus point is moved to the midpoint of both edges, which is the center of the droplet in a horizontal plane. The radial position of measurement is determined as the displacement of the x-axis stage. Strictly, we need to take into account of the change in refractive index for an accurate determination of the vertical position in a droplet, though refractive index of test fluid may not be uniform and may change during drying. However, for the position near the surface or bottom, we actually neglected the effect of refractive index and the focus point was just moved by a desired distance from the droplet surface or glass plate using the z-axis stage. In contrast, the measurement position of the middle height was determined as a midpoint between the droplet surface and glass plate being detected through the concentrated test fluid. The viscosity measurement was carried out using a single magnetic sphere observed in the microscopic image at the horizontal and vertical positions as described above.

Results and Discussion

Characterization of drying process based on the change of droplet dimension

We firstly showed the change of droplet size during drying in order to check the reproducibility of drying process and to discuss the difference of drying rate. Figure 3 shows the changes of the

height, diameter, and volume of drying droplet. The data obtained at the same droplet volume (3 or 7 μL) and drying condition (180 or 300°C of heater temperature, or room temperature) are expressed by the same plots. Good reproducibility in drying experiment can be confirmed by relatively small error in each plot. Since the droplet height was decreased at a roughly constant rate and the diameter was decreased as a square root function of time, the volumetric drying rate was then constant throughout drying. Also, volumetric drying rate was not significantly changed with the initial volumes of droplet.
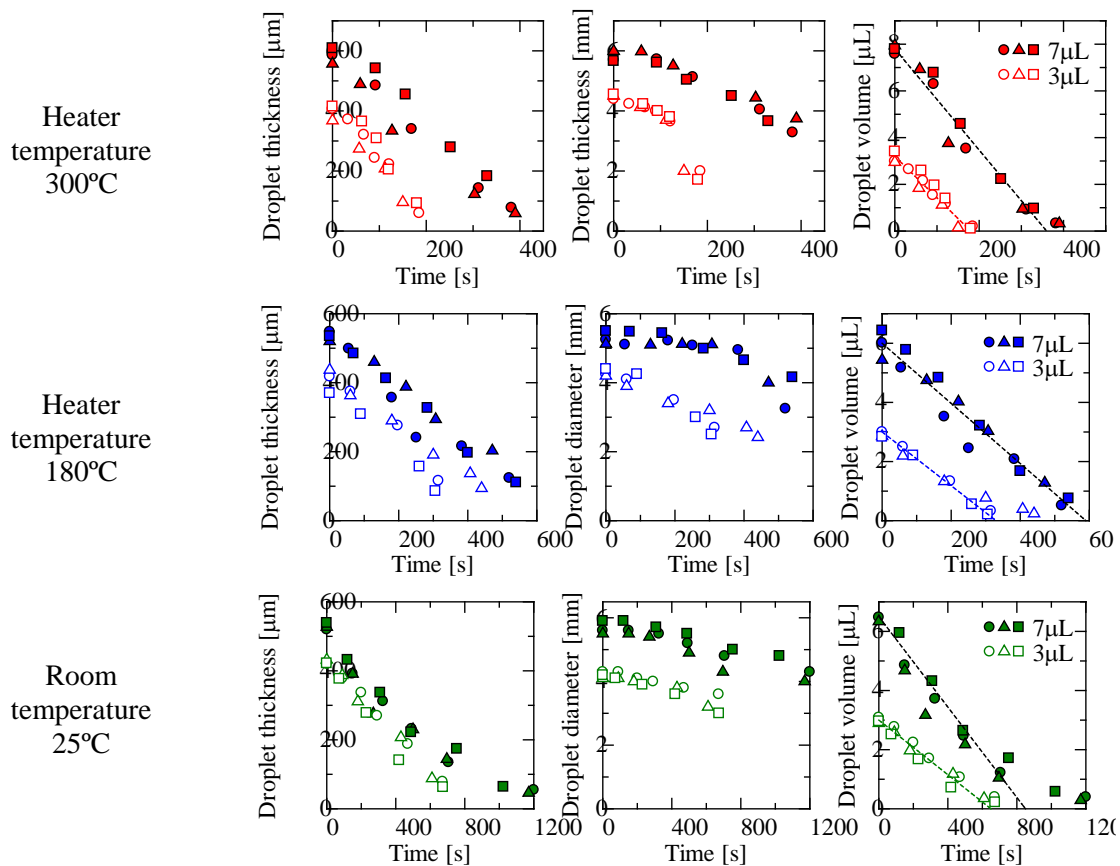

Figure 3 Change of the dimensions and volume of droplets during drying

Vertical distribution of local viscosity in a drying droplet

In this section, the change of local viscosity at different vertical positions and at the center of drying droplet in the horizontal plane is discussed. The measurement of local viscosity change was performed three times at different vertical positions using a 7μL droplet under different drying conditions. The vertical positions for measurement are 1) 50μm below the droplet surface (Surface), 2) at the middle height of droplet (Middle), and 3) 50μm above the glass cell (Bottom). Since the vertical positions of magnetic particle and marker particle on the droplet surface were alternately measured, the magnetic particle of interest may not be identical for each measurement. Therefore, Bottom position was fixed during drying, while others were lowered as drying proceeds.

Figure 4 shows the change of local viscosity as functions of droplet volume.   At 300°C of

heater temperature, local viscosity near the surface showed gradual increase, meanwhile those near the bottom and at the middle height of droplet were initially decreased and followed by a slight increase in the latter stage of drying. Initial viscosity decrease is probably caused by temperature decrease due to conductive heating from the glass cell heated by NiCr heater. As a result, it is demonstrated that noticeable viscosity gradient was locally formed near the surface of the droplet and viscosity was kept uniform beneath the surface. The result indicates the local concentration of test fluid or the formation of skin layer at the drying surface. As a future work, viscoelastic measurement is indispensable for characterizing the mechanical properties of the skin layer.

On the other hand, when drying at 180ºC of heater temperature or at 25ºC of room temperature, no significant increase in viscosity were observed in the early stage of drying at any positions, but the viscosity began to increase when the droplet volume was decreased by half. After this point, the viscosity only near the surface was preferentially increased at the heated condition, while the viscosities at any positions were uniformly and slowly increased at natural drying condition. Therefore, it was revealed under weakly heated condition that PVA solution was initially concentrated uniformly and was started to be locally concentrated in the middle stage of drying, probably due to the decrease in molecular diffusivity. On the contrary, PVA solution kept uniform almost till the end of drying under sufficiently slow drying condition.
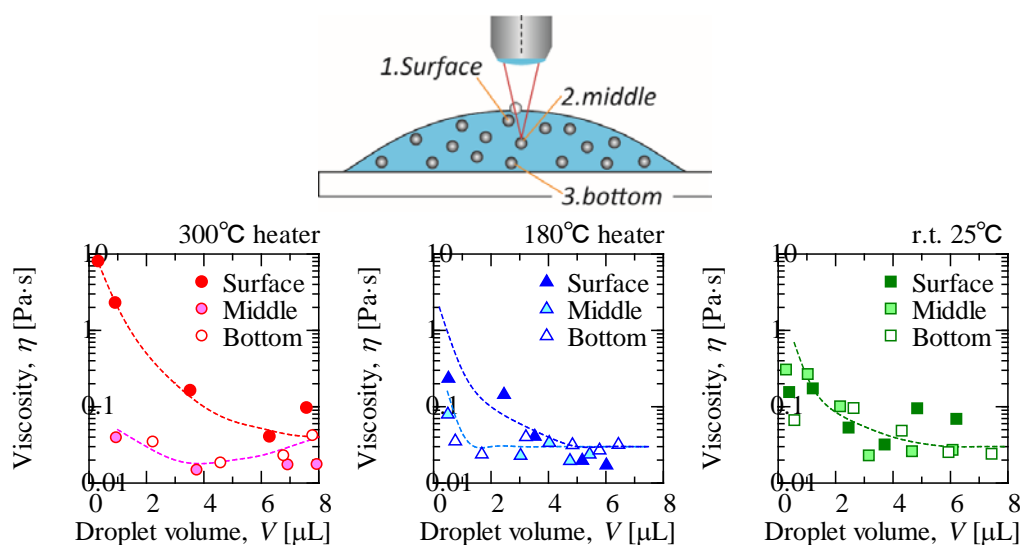

Figure 4 local viscosity change at different vertical positions in a drying droplet

Horizontal distribution of local viscosity in a drying droplet

We also investigated the difference of local viscosity change at different horizontal positions and discussed the generation process of viscosity distribution in the drying droplet. The viscosity measurement at different radial distances from the center of a 7μL droplet was performed at each drying condition. The vertical position was constant at 50μm from the glass cell, and the horizontal positions are A) near the edge of the droplet (Edge), B) at the midpoint between the edge and center (Middle), and C) at the center (Center), which is identical with position 3) described in the

previous section. Although the thickness of droplet at the periphery was too thin to measure particle motion without the effect of glass cell, position A) was actually 0.2mm from the periphery of droplet, where the droplet thickness was more than 60μm. As seen in Figure 2, the distance between positions A) and C) or the base radius of droplet was decreased from 3mm to 2mm. Therefore, position C) was fixed during drying, while others moved inward as drying proceeds.

The viscosity change at each position under different drying conditions are shown in Figure 5. At 300ºC of heater temperature, viscosity near the edge was initially increased and then became constant. Since position A) was actually move inward as decreasing droplet diameter, the initial viscosity increase near the edge indicates that concentrated region expanded more rapidly than the shrinkage of droplet diameter. The subsequent constant viscosity term suggests that the concentrated region is fully developed around the periphery. As for positions B) and C), local viscosity was slowly increased in the latter stage of drying similar to that at vertical positions beneath the droplet surface. After a while, local viscosity was successively increased in the order of position B) and C) presumably because the boundary of the concentrated region proceeded inward. When local viscosity began to increase at position B), the distance from the edge to position B) was roughly 1.2mm, which corresponds to the thickness of the concentrated region.

On the other hand, at 180ºC of heater temperature local viscosities at positions A) and B) were simultaneously increased in the middle of drying, while showing constant viscosity at the center. The concentrated region was also generated from the edge under slow drying condition. Fully development of the concentrated region was evidenced by constant viscosities at A) and B) just before the end of drying. However, no initial viscosity increase at the edge suggest that the concentrated region was quite thin. As drying proceeds, positions A) and B) were sufficiently close and the concentrated region was expanded. Therefore, it is deduced that A) and B) located in the concentrated region almost at the same time, resulting in a simultaneous increase in viscosity.
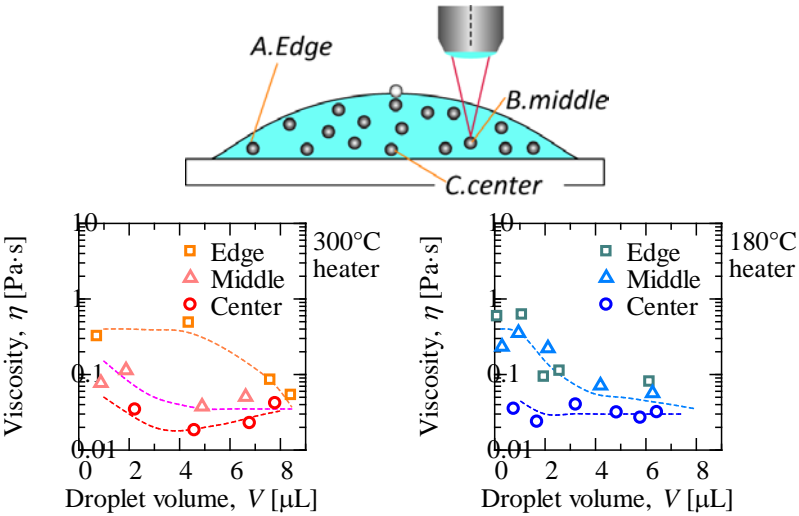

Figure 5 local viscosity change at different horizontal positions in a drying droplet

Effect of droplet volume on the vertical distribution of local viscosity

Localization of non-volatile component in a drying droplet is restrained by the diffusion of the component and convective flow in a droplet. At higher drying temperature, less viscous fluid enhanced fluid flow in a droplet and Marangoni convection owing to inhomogeneous distribution of concentration on the surface assist the homogenization, while large shrinking rate accelerates the formation of skin layer. In the current experimental conditions, Figure 2 indicates that the decreasing rates of thickness and volume of droplet were not drastically changed for smaller droplet compared to large one. Therefore, smaller droplet was dried up in a short time, and did not have sufficient time to homogenize the materials in the droplet. Therefore, we investigated the distribution of local viscosities in the vertical direction of a smaller droplet. Figure 6 shows the change of local viscosity at different vertical positions in a 3μL droplet. The definition of vertical positions is identical with 7μL droplet.

At 300ºC of heater temperature, local viscosity near the surface were gradually increased from the very early stage of drying similar to 7μL droplet case. In contrast, those at the middle and near the bottom showed slight decrease in the former part of drying and then both were sharply increased before the end of drying. Although the viscosity difference at the intermediate stage of drying is larger than a large droplet case, the formation of skin layer was confirmed as expected for a smaller droplet. Additionally, very large viscosities at all vertical positions just before the end of drying means that magnetic particles used for these measurements were all located in a skin layer, which is now fully developed throughout the droplet. Interestingly, similar trend in the change of local viscosity at any vertical positions was observed in a 3μL droplet dried at 180ºC of heater temperature. Therefore, it is revealed that similar material localization was observed even at different heating conditions for smaller drying droplets.

In contrast, at the natural drying condition of 25ºC, no significant difference in viscosity change was observed among vertical positions and the viscosity started to be increased at the droplet volume of 2μL. We also found that local viscosities are increased in the similar manner regardless of droplet volume and measurement position if the droplet volume was normalized by its initial value. Therefore, it is concluded that drying process of PVA solution droplet was not affected by droplet volume when drying at room temperature.
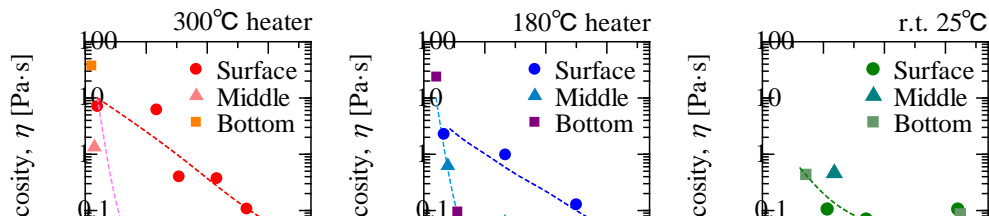

Figure 6 Effect of initial volume on the local viscosity change in the drying droplet

Discussion on the viscosity distribution from the view point of dimensionless numbers

In a drying droplet, Marangoni convection is one of the influential factors to restrain material localization. It was reported that fluid flow in a droplet is governed by Marangoni convection when Marangoni number, Ma, is larger than 80[11]. The definition of Ma is expressed as Eq. (5).

$$\mathrm{Ma} = \frac{\Delta \gamma a}{\rho v \alpha} \qquad (5)$$

where, $\Delta \gamma$, ρ, v, α represent surface tension difference along droplet surface, density of test fluid, kinematic viscosity of test fluid and thermal diffusivity. Also, it was reported that Marangoni convection is dominant in a droplet having contact angle larger than 20°[11]. In the present study, the critical condition for generating Marangoni convection is $\Delta \gamma < 5 \times 10^{-3}$ mN/m, which corresponds to that the temperature difference on droplet surface is smaller than the order 0.03K. Additionally, the contact angle of droplet, being calculated from the thickness/diameter ratio, in the current system was changed from 20° to 10° as drying proceeds. Therefore, although Marangoni convective flow must be generated in a droplet, the effect of the flow to homogenize the material distribution became negligible due to the flattened shape of droplet in the latter stage of drying.

Considering the different behavior of local viscosity change between droplet volumes at 180ºC of heater temperature, whether the polymer solution keep uniform or not during drying may be affected by thinning rate of droplet and diffusion rate of solute. We thus introduced Peclet number being the ratio of the film shrinking rate to solute diffusion rate as defined by Eq. (6).

$$Pe = \frac{\frac{1}{\pi a_{1/2}{}^2} \frac{dV}{dt} h_{1/2}}{D} \qquad (6)$$

where, $a_{1/2}$ and $h_{1/2}$ represent the base radius and thickness of droplet when its volume was reduced by half, and D the diffusion coefficient of solute in water. Diffusion coefficient of PVA molecules in a dilute solution at 25ºC was measured as 4×10^{-11} m^2/s and that at different temperatures was calculated using Arrhenius equation with the activation energy $\Delta E = 30.5$ kJ/mol [12].

Table 1 Peclet number at each drying condition and droplet volume

Initial droplet volume	300˚C	180˚C	r.t. 20˚C
7μL	5.2	3.1	2.3
3μL	5.3	5.3	2.4

In the case of heater drying, the measured surface temperature of liquid film having the thickness of 1mm using an infrared thermometer was used to calculate diffusion coefficient; 30ºC and 40ºC for 180ºC and 300ºC of heater temperatures. Peclet number calculated at each experimental condition is shown in Table 1. It is clearly shown that the formation of skin layer was observed just after the start of drying only at $Pe > 5$, where the relative shrinking rate is sufficiently

larger than PVA diffusion. In contrast, the droplets were uniformly concentrated at $Pe \approx 2$, and the skin layer was generated at the latter part of drying at an intermediate Peclet number condition.

Conclusion

In the present study, we developed the system to measure local viscosity at the point having the volume of several pico-litter in transparent materials. The measurement system was then applied to the drying process of a sessile droplet of PVA aqueous solution. When the droplet dried quickly using a 300ºC heater, it is elucidated that local viscosity at the surface was preferentially and monotonically increased regardless of droplet volume, while keeping constant viscosity beneath the surface. Such a viscosity distribution corresponds to the formation of skin layer at the surface. The horizontal viscosity distribution clearly showed that the concentrated region along the periphery of droplet was first formed and expanded inward. In contrast, no viscosity distribution was observed in a droplet when drying at room temperature. On the contrary, under a moderate drying condition using a 180ºC heater, the variation of local viscosity was affected by initial droplet volume. That is, skin layer formation was easily observed for a smaller droplet, while local viscosity at the surface was solely increased in the latter stage of drying for a larger one. Horizontal viscosity distribution implies the existence of thin concentrated region at the edge. Parameter analysis on the current investigation shows that Marangoni convective flow was basically restrained in the latter stage of drying due to small contact angle and that the distribution of local viscosity was reasonably explained by Peclet number, being the ratio of droplet shrinkage to PVA molecule diffusion.

Reference

1) P. E. Price, Jr., R. A. Caironcross, *J. App. Polym. Sci.*, **2000**, 78, 149-165
2) R. K. Arya, T. Kshitij and S. Sakshi, *Prog. Org. Coat.*, **2016**, 95, 8-19
3) S. Lim, KH. Ahn, M. Yamamura, *Langmuir*, **2013**, 29(26), 8233-8244
4) A. Pommella, V. Preziosi, S. Caserta, J. M. Cooper, A. Guido, M. Tassieri, *Langmuir* **2013**, 29, 9224−9230
5) K. Sakai, Y. Yamamoto, *Applied physics letters*, **2006**, 89, 211911
6) JO. Song, R.M. Henry, R.M. Jacobs, L.F. Francis, *Rev. Sci. Instruments* **2010**, 81, 093903
7) JO. Song, A.V. McCormick, L.F. Francis, *Macromol. Mater. Eng.*, **2013**, 298, 145–152
8) JC. Kim, M, Seo, M. A. Hillmyer, L. F. Francis, *ACS Appl. Mater. Interfaces*, **2013**, 5(22) 11877-11883
9) Y. Komoda, L.G. Leal, T. M. Squires, *Langmuir* **2014**, 30, 5230−5237
10) Z. Wang and Y.P. Zhao, J. *Adhesion Sci. Technol.* **2011**, DOI:10.1163/156856111X600523
11) H. Hu and R. G. Larson, *Langmuir* **2005**, 21, 3972-3980
12) M. Okazaki, K. Shinoda, K, Masuda, R. Toei, *J. Chem. Eng. Japan*. **1974**, 7, 99−105